

Quantized light lenses for atoms: The perfect thick lens

B. Rohwedder and M. Orszag

Facultad de Física, Pontificia Universidad Católica de Chile, Casilla 306, Santiago 22, Chile

(Received 16 July 1996)

A cylindrical light lens for atoms is studied in the limit of high detuning. The dynamics of atomic motion in a quantized electromagnetic field is shown to be separable into strictly classical and purely quantum-mechanical aspects when an ideal lens of arbitrary thickness is assumed. New insight is gained in the thick-lens regime, both in the classical and quantal domain. Different sources of aberration in nonideal lenses are studied. Their inclusion in a subsequent feasibility discussion for the observation of focal structures caused by field quantization sets experimental tolerances for an eventual measuring apparatus. [S1050-2947(96)08112-7]

PACS number(s): 03.75.Be, 32.80.Lg, 42.50.Vk

I. INTRODUCTION

Recent advances in the field of atom optics have demonstrated several techniques for manipulating neutral atom beams. In particular, since the first realization of a convergent lens for atoms [1], a wide range of focusing schemes has been conceived and concretized experimentally, among them radiation pressure force- [2], Fresnel- [3], and magnetic hexapole [4] lensing. The first demonstration of atomic beam focusing with laser light was however based on the dipole force and made use of a red detuned TEM_{00} laser beam that caused the copropagating near-resonant atoms to be attracted to its center [5]. A similar technique using a blue detuned TEM_{01}^* mode has been proposed in order to minimize spontaneous forces by attracting the atoms to the zero field at the donut-laser core [6]. Alignment problems are less severe when the atomic beam intersects a standing laser field orthogonally, but the ideal, i.e., parabolical shape of the optical potential will only be realized close to the maxima (minima) of the red (blue) detuned standing light wave. Such a cylindrical lens potential can have quite a large period, if formed above a mirror by reflection at a near-grazing incidence angle. With a single period of such a lens, imaging of a microstructure was demonstrated for the first time [7]. Multiple periods can be used as an array of cylindrical lenses, which focus the incoming atomic beam into a parallel set of lines. By depositing these onto a substrate, a lithographic technique was created [8–10]. For an appropriate choice of relative phases and polarizations, a pair of orthogonal linearly polarized standing waves forms a two-dimensional array of atom lenses and could be used for depositing a high number of identical, arbitrary patterns onto a substrate [11].

The recent observation of multilevel effects in direct-write lithography using Cr atoms [12] shows that the present state of the art is in need of a deeper understanding of the basic interaction of atoms with near-resonant light. As an example for a useful extension of two-level atomic models, we mention here the recently proposed possibility of improving the parabolic shape of standing-wave optical potentials by making use of a three-level configuration [13]. The description of the external degree of freedom can be improved as well, by going beyond ordinary particle optics. For some lens configurations, both corpuscular and wave-mechanical descriptions have already been developed [6,10], thus allow-

ing the estimation of diffractive limits for the focal spot size. Also the modeling of the light field has been enhanced. In their seminal paper [14], Averbukh, Akulin, and Schleich predict a focal substructure caused by the quantal nature of a thin light lens for two-level atoms in the limit of high detuning.

In the present paper we show that even under extreme experimental conditions, the influence of light quantization on the detailed focal shape of perfect atomic light lenses can be completely ignored in the classical limit.

Here is a brief outline. After specifying the system we are interested in and proposing a dynamic model for its description, the essentials of the atomic focusing process are studied in detail. Under these idealized conditions a clean separation of “classical” ray-optical and “quantum” wave optical properties is possible, thus establishing a very intuitive relation among the usual atom-optical viewpoint [16] and the results presented in [14,15]. Expressions describing the size of the “classical” focus (disregarding details imposed by the given photon statistics) are derived as well as the geometry of the “quantal” focal distribution. Since we deal with a parabolic lens of arbitrary thickness (with obvious restrictions on the interaction time imposed by diffusive aberration) it becomes possible to study the thick-lens regime. On the classical level and contrary to what one would naively expect by extrapolating thin-lens results, we find that our atom lens should become divergent for high enough laser intensities. On the quantum level, an interesting “eight”-shaped distribution of foci over the focal plane is found. In Sec. V the strict physical conditions imposed so far are relaxed and various sources of aberration are studied. The stage is then set for discussing the observability of focal details imposed by the quantum nature of light. A simple criterion is given and tested using very extreme, recently achieved experimental parameters [25]. After a quantitative estimation of the maximal tolerances that an eventual measuring apparatus would have to fulfill, the paper closes with the proposition of several observational schemes.

In order to ease the comparison with prior work, we decided to keep as close as possible to the notational conventions introduced in [15].

II. THE MODEL

We consider a tightly collimated beam of neutral atoms of mass M that moves in the x - z -plane along $x = \kappa z > 0$. We will

assume that the atoms are prepared in such a way, that they can be well described as two-level systems with a characteristic transition energy $\hbar\omega_a$. In the interaction region $-L < z < 0$, the atoms cross an orthogonal one-mode standing light wave detuned by an amount $\Delta \equiv \omega_a - \omega$ from the atomic resonance. The velocity v_z of the atoms along the beam axis (z axis) is considered to be sufficiently large so that the spatial dependence of the electromagnetic field along z can be replaced with the explicit time dependence $t = z/v_z$. For the sake of simplicity the system is assumed to be uniform in the y direction, i.e., we are analyzing the properties of a cylindrical quantum light lens.

Under these circumstances, the physical problem effectively reduces to analyzing the quantum dynamics of a two-level system moving in one dimension (x axis) and interacting with one mode of a given, quantized electromagnetic field. If $|+\rangle$ and $|-\rangle$ denote the upper and lower atomic states, respectively, the extended Jaynes-Cummings Hamiltonian describing this situation reads

$$H = \hbar\omega a^\dagger a + \frac{\hbar\omega_a}{2} \sigma_z + \frac{p_x^2}{2M} + \hbar[a\sigma_+ g(x) + a^\dagger \sigma_- g^*(x)], \quad (2.1)$$

where $\sigma_z \equiv |+\rangle\langle+| - |-\rangle\langle-|$, $\sigma_+ \equiv |+\rangle\langle-| = \sigma_-^\dagger$ and the pair x, p_x of complementary operators $[x, p_x] = i\hbar$ describes the atomic motion along x . The one mode of the electromagnetic field is represented by the operators a and a^\dagger , $[a, a^\dagger] = 1$, and by its space dependence which is included, together with the electric dipole moment of the atomic transition, in the coupling constant $g(x)$. Outside the interaction region $g(x) \equiv 0$, of course.

We will concentrate on the limiting case of high detuning, for which Eq. (2.1) reduces to the effective Hamiltonian [17]

$$H_{\text{eff}} = \hbar\omega a^\dagger a + \frac{\hbar\omega_a}{2} \sigma_z + \frac{p_x^2}{2M} + \frac{\hbar|g(x)|^2}{\Delta} \sigma_z a^\dagger a. \quad (2.2)$$

In this limit, the atoms remain in their initially prepared internal state, which we will assume to be $|-\rangle$. If this is a true ground state, spontaneous emission plays no role at all. More realistically, however, for a given interaction time $T = L/v_z$ there exists a nonvanishing probability of finding the atom in its excited level and one has to operate sufficiently far from resonance in order to keep the average number of spontaneous decays well below one. We will assume such conditions and thus neglect diffusive aberrations in this paper.

III. ESSENTIALS OF THE FOCUSING PROCESS

A. The perfect lens

First of all we want to learn about the basic physics involved in the focusing process. For this purpose we will make some further assumptions about our system. In the spirit of [18] ‘‘rather than confuse the physical results by mathematical complexity, we shall set up a different, but analogous, expression which leads to a simpler mathematical form.’’ This is why we will imagine that the collimation of the atomic beam is accomplished with a *Gaussian* (instead of a rectangular) slit of width d . On the contrary, the usually Gaussian laser-beam profile will be modeled as *rectangular*

and of width L . Experimentally we will usually encounter sinusoidal standing waves and we will therefore assume

$$g(x) = G \sin\left(\frac{2\pi x}{\lambda}\right). \quad (3.1)$$

Since spontaneous forces are smaller in regions of low-field intensity, we will expand $|g|^2$ up to quadratic order,

$$|g(x)|^2 \approx \left(\frac{2\pi G}{\lambda}\right)^2 x^2, \quad (3.2)$$

around a field intensity minimum and require $\kappa, d \ll \lambda/4$. This situation is in the spirit of [7,16] and should be contrasted with the more usual situation, in which the atomic beam width is much larger than the standing-wave period employed.

If we expand the quantum-mechanical states in the product basis,

$$\sum_{j=-,+} \sum_{n=0}^{\infty} \int_{-\infty}^{\infty} dx' |j, n, x', t\rangle \langle j, n, x', t| = 1, \quad (3.3)$$

$$\langle j, n, x', t | k, m, x'', t \rangle = \delta_{jk} \delta_{nm} \delta(x' - x''), \quad (3.4)$$

of eigenstates of σ_z , $a^\dagger a$, and x , the Schrödinger equation corresponding to Eq. (2.2) decouples into a set of equations for each photon number $n=0,1,2,\dots$. Because of the initial condition selected, the atoms remain in their lower state all the time. Thus for $\Delta < 0$ we get a simple harmonic-oscillator problem,

$$i\hbar \frac{d}{dt} \langle -, n, x', t | \psi \rangle = \langle -, n, x', t | \hbar\omega n - \frac{\hbar\omega_a}{2} + \frac{p_x^2}{2M} + \frac{M\omega_n^2 x^2}{2} | \psi \rangle, \quad (3.5)$$

for each n , whose angular frequency is given by

$$\omega_n^2 = -\frac{2\hbar}{\Delta M} \left(\frac{2\pi G}{\lambda}\right)^2 n. \quad (3.6)$$

B. Initial conditions and solution

In a real experiment, the lateral velocity of the atoms before entering the interaction region will in general not exactly equal zero. On the one hand, the orthogonal beam-beam alignment is only possible within certain experimental margins. On the other hand, mechanical vibrations of the standing wave relative to the atomic beam and its nonvanishing transverse temperature will cause fluctuations both in κ and in the initial lateral momentum \wp . For these reasons we will assume that just before entering the standing light field, the system is described by

$$\langle -, n, x', -T | \psi \rangle = w_n \frac{1}{\sqrt{\sqrt{\pi}d}} \exp\left[-\frac{1}{2} \left(\frac{x' - \kappa}{d}\right)^2 - \frac{i}{\hbar} \wp(x' - \kappa)\right], \quad (3.7)$$

where $\Sigma_0^\infty w_n |n\rangle$ is the electromagnetic field photon statistics. (Because of our lack of information about the single atom in a beam, the center-of-mass motion should in fact be described by a statistical operator, as pointed out in [19]. In the name of conceptual simplicity, here we will, however, stick with the popular bias and describe the initial atomic state as a pure one, i.e., by a Schrödinger wave function). Doppler shifts and the corresponding velocity-dependent forces can be neglected, as will become apparent *a posteriori* when we discuss the restrictions that have to be imposed on the magnitude of φ .

The dynamics of a Gaussian wave packet in a harmonic-oscillator potential is well known [20]. After traversing the interaction region, the atom is ‘‘released’’ and moves freely again. By applying the free propagator and computing the squared modulus of the resulting wave function for $t > 0$, one gets the time-dependent Gaussian

$$\begin{aligned} & |\langle -, n, x', t | \psi \rangle|^2 \\ &= \frac{|w_n|^2}{\sqrt{\pi} D_n(t)} \exp \left\{ - \left[\frac{x' - x'_n(T) + v'_n(T)t}{D_n(t)} \right]^2 \right\}, \end{aligned} \quad (3.8)$$

whose width $D_n(t)$ is given by

$$\begin{aligned} D_n(t) \equiv & d \left[\left(\frac{\hbar}{d^2 M \omega_n} \right)^2 (\omega_n t \cos(\omega_n T) + \sin(\omega_n T))^2 \right. \\ & \left. + (\cos(\omega_n T) - \omega_n t \sin(\omega_n T))^2 \right]^{1/2}. \end{aligned} \quad (3.9)$$

Assuming $\varphi=0$ and by a different method, a similar¹ expression has been obtained in [15]. With the introduction of the quantities $x'(T)$ and $v'(T)$ in Eq. (3.8) we are led to an extremely simple physical picture. Let a classical mass point M be subjected to the Hamiltonian

$$H_{\text{cl}} = \frac{p'^2}{2M} + \frac{M\omega^2 x'^2}{2}, \quad (3.10)$$

with the initial conditions $x'(0) = \kappa$ and $p'(0) = \varphi$. The coordinate and momentum of the particle after a time T are given by

$$x'(T) = \kappa \frac{\cos(\omega T + \phi)}{\cos \phi}, \quad (3.11)$$

$$p'(T) = \varphi \frac{\sin(\omega T + \phi)}{\sin \phi} = Mv'(T), \quad (3.12)$$

where

$$\tan \phi \equiv \frac{\varphi}{M\omega\kappa}. \quad (3.13)$$

Since in Eq. (3.5) the potentials involved are not ‘‘worse’’ than quadratic, it is no surprise to find essentially classical

features also in the quantum-mechanical result (3.8): After bouncing back and forth inside the harmonic pot, the atomic wave packet is suddenly released at $t=0$ and, as the explicit calculation shows, continues moving straight as would be expected from a classical object.

C. Two kinds of foci

This classical behavior can be well described in terms of effective ‘‘dipole forces’’ and has already been thoroughly studied in the context of atomic beam focusing and manipulation. Observe that the n th wave-packet trajectories,

$$x' = x'_n(T) - v'_n(T)t, \quad (3.14)$$

of all parallel (and paraxial, i.e., $|\phi| \ll 1$) incoming atoms intersect each other at exactly one point,

$$\begin{pmatrix} x_n^{\text{CF}} \\ z_n^{\text{CF}} \end{pmatrix} = \begin{pmatrix} -\frac{\varphi}{M\omega_n} \csc(\omega_n T) \\ \frac{v_z}{\omega_n} \cot(\omega_n T) \end{pmatrix}, \quad (3.15)$$

which is thus a focal spot (actually a focal line along y) of this cylindrical atomic lens. We will call it a *classical* focus, since most of the involved physics can be readily understood semiclassically and described using geometrical optics. Its width is given by

$$D_n(t_n^{\text{CF}}) = \frac{\hbar}{dM\omega_n} \frac{1}{|\sin(\omega_n T)|}. \quad (3.16)$$

It will now be convenient to introduce the dimensionless parameter

$$\alpha \equiv \frac{d^2 M}{\hbar T} \quad (3.17)$$

and the short form $\varphi_n \equiv \omega_n T$. A clumsy way of writing the beam width (3.9),

$$\begin{aligned} D_n(t) = & d \left[\left(\frac{\cos^2 \varphi_n}{\alpha^2 \varphi_n^2} + \sin^2 \varphi_n \right) (\omega_n t - \omega_n t_n^{\text{QF}})^2 \right. \\ & \left. + \frac{1}{\cos^2 \varphi_n + \alpha^2 \varphi_n^2 \sin^2 \varphi_n} \right]^{1/2}, \end{aligned} \quad (3.18)$$

makes evident both its symmetry around

$$\omega_n t_n^{\text{QF}} \equiv \sin \varphi_n \cos \varphi_n \frac{\alpha^2 \varphi_n^2 - 1}{\cos^2 \varphi_n + \alpha^2 \varphi_n^2 \sin^2 \varphi_n} \quad (3.19)$$

and its linear growth for $|t| \rightarrow \infty$ which, by extrapolating the asymptotes, seems to indicate beam convergence at the position $z_n^{\text{QF}} = v_z t_n^{\text{QF}}$, where D_n in fact becomes minimal, thus defining a *quantal* focus for the n th partial Schrödinger wave. Its width is given by

$$D_n(t_n^{\text{QF}}) = \frac{d}{\sqrt{\cos^2 \varphi_n + \alpha^2 \varphi_n^2 \sin^2 \varphi_n}}. \quad (3.20)$$

If we restrict ourselves to photon numbers

¹See the discussion in the section about spherical aberration.

$$n > \frac{\hbar(-\Delta)}{2d^4M} \left(\frac{\lambda}{2\pi G} \right)^2, \quad (3.21)$$

we get $\alpha\varphi_n > 1$ and thus

$$D_n(t_n^{\text{QF}}) < d, \quad (3.22)$$

i.e., the quantal foci are narrower than the initial beam width.

IV. CLASSICAL AND QUANTAL PROPERTIES

A. Thin vs thick lenses

In many experiments, the trajectories of the particles are usually only slightly curved by the optical potential. In our context, this condition means that $\varphi_n \ll 1$ must hold for all relevant n values, and we will call it the thin-lens condition. According to Eq. (3.15), in this limit the rays coming in with identical φ but different κ all intersect at

$$\begin{pmatrix} x_n^{\text{CF}} \\ z_n^{\text{CF}} \end{pmatrix} \approx \frac{1}{\varphi_n^2} \begin{pmatrix} -\varphi/M \\ v_z \end{pmatrix} T, \quad (4.1)$$

which means that the focal length z_n^{CF} decreases as $1/n$.

If we further assume ‘‘classical light,’’ i.e., a coherent state

$$|w_n|^2 = \frac{\langle a^\dagger a \rangle^n}{n!} e^{-\langle a^\dagger a \rangle} \quad (4.2)$$

with large $\langle a^\dagger a \rangle$, the single classical foci corresponding to each n will be distributed over a distance characterized by the width $\langle a^\dagger a \rangle^{1/2}$ of Eq. (4.2), i.e.,

$$\frac{(-\Delta)Mv_z}{2\hbar T} \left(\frac{\lambda}{2\pi G} \right)^2 \frac{1}{\langle a^\dagger a \rangle^{3/2}}, \quad (4.3)$$

which provides an order-of-magnitude estimation for the size (in the z direction) of the focal spot which is centered at

$$z_{\langle a^\dagger a \rangle}^{\text{CF}} = \frac{(-\Delta)Mv_z}{2\hbar T} \left(\frac{\lambda}{2\pi G} \right)^2 \frac{1}{\langle a^\dagger a \rangle}. \quad (4.4)$$

If $\varphi=0$, the focal spot width in the x direction is approximately given by

$$D_{\langle a^\dagger a \rangle}(t_{\langle a^\dagger a \rangle}^{\text{CF}}) = \frac{(-\Delta)}{2dT} \left(\frac{\lambda}{2\pi G} \right)^2 \frac{1}{\langle a^\dagger a \rangle}, \quad (4.5)$$

which does not contain \hbar nor the atomic mass M anymore. As a consequence of Eq. (4.1), fluctuations of the initial lateral momentum φ will widen the spot in the x direction beyond the diffraction limit (4.5). Fluctuations of κ will broaden it additionally due to the shifts (5.5) and (5.6) caused by spherical aberration.

The thin lens is intrinsically convergent. As can be seen in Eq. (3.15), this behavior will, however, change as we increase $\langle a^\dagger a \rangle$. As soon as $\varphi_n > \pi/2$ (‘‘thick-lens’’ regime), the classical focal length will become negative and the lens a divergent one. (For even larger intensities and as long as the entire model keeps its validity, the lens should become convergent again, etc.) In terms of the classical picture given at the end of Sec. III B this result is not at all surprising. It

could in principle be observed with a scheme similar to the one described in [16]. Note however that using the parameters leading to Fig. 2 of that paper, the critical condition $\omega_{\langle a^\dagger a \rangle} T = \pi/2$ corresponds to an unrealistically high (cw) laser power of ~ 15 W. Obviously a better suited transition and a higher coupling constant will be needed for demonstrating the transition from the convergent into the divergent focusing regime.

B. The quantum focal curve

The focal curve in the x - z plane is obtained by introducing Eq. (3.19) into the trajectory (3.14) and can be conveniently rationalized via

$$\begin{pmatrix} x_n^{\text{QF}} \\ z_n^{\text{QF}} \end{pmatrix} \equiv \begin{pmatrix} \kappa \xi_n \\ \alpha L \zeta_n \end{pmatrix}. \quad (4.6)$$

This parametrized focal curve has a surprisingly simple structure, since one can show that for large α it rapidly approaches the asymptotical form

$$\left(|\xi_n| - \frac{1}{2} \right)^2 + \zeta_n^2 = \frac{1}{4} \quad (4.7)$$

with growing n . The condition (4.7) defines the double circular lobe depicted in Fig. 1. The stretching factors αL and κ depend solely on properties of the atomic beam. While the x amplitude equals its initial lateral shift, the amplitude in z is proportional to the momentum of the atoms in this direction and the square of its width.

An example for the distribution of the individual foci along this curve for different values of α is also included in Fig. 1. Already for $\alpha=1$ the foci concentrate mainly along the central tangent at $x \approx 0$ and only very close to $\varphi_n \equiv m\pi$, $m=0,1,2,\dots$ will they be found far away from the z axis. (From the inequality (4.8) it follows that this becomes increasingly true with growing n .) Again, as in the classical case, we observe that for some n we get unphysical (‘‘virtual’’) foci at negative t_n^{QF} . The relation among the two kinds of foci will be analyzed in Sec. IV C.

C. Relation among classical and quantal foci

Let us assume $\alpha\varphi_n \geq 1$. One then easily checks that $|t_n^{\text{CF}}| \geq |t_n^{\text{QF}}|$ and that classical and quantal foci become real (virtual) for the same value of n . Since they both lie on the trajectory line (3.14), it is geometrically evident that they should essentially coincide in position when close to the z axis. This is the case when the condition $\alpha^2 \varphi_n^2 \sin^2 \varphi_n \gg |\cos \varphi_n|$, or equivalently

$$\frac{|\cos \varphi_n|}{\varphi_n^2 \sin^2 \varphi_n} \ll \alpha^2 \quad (4.8)$$

is fulfilled, since we then get

$$|x_n^{\text{QF}}| \ll \kappa. \quad (4.9)$$

Classical and quantal foci will then be equally distributed,

$$z_n^{\text{QF}} \approx v_z T \frac{\cos \varphi_n}{\varphi_n \sin \varphi_n} \approx z_n^{\text{CF}}, \quad (4.10)$$

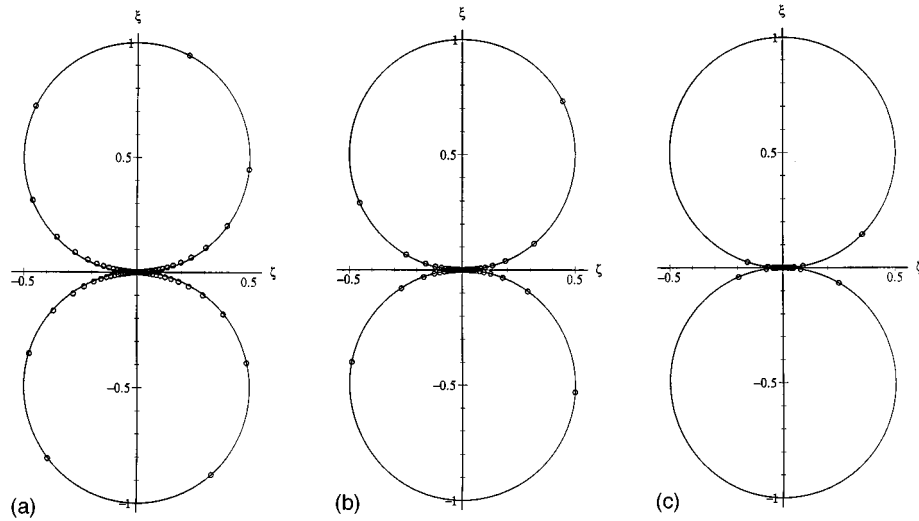


FIG. 1. Illustrative examples of the quantum focal distribution for $\alpha=0.4$ (a), $\alpha=1$ (b), and $\alpha=4$ (c). In (a) a slight deviation from the asymptotic form (4.7) can be noticed. In realistic situations $\alpha \gg 1$ and essentially all the foci concentrate close to the origin.

and we will introduce the superscript F as a short form for referring to both.

In the case of thin lenses and, more generally, whenever $|\varphi_n - m\pi| \ll 1$ holds for a given $m=0,1,2, \dots$ but Eq. (4.8) is still fulfilled, the positions (4.10) simplify to

$$z_n^F \approx \frac{L}{\varphi_n} \frac{1}{\varphi_n - m\pi}, \quad (4.11)$$

and the distance between two consecutive foci, when n is large, becomes

$$z_n^F - z_{n+1}^F \approx \frac{L}{n} \frac{1}{(\varphi_n - m\pi)^2}. \quad (4.12)$$

Correspondingly, whenever $|\varphi_n - (m+1/2)\pi| \ll 1$, we get

$$z_n^F \approx \frac{L}{\varphi_n} [\pi(m+1/2) - \varphi_n], \quad (4.13)$$

and

$$z_n^F - z_{n+1}^F \approx \frac{L}{2n} \quad (4.14)$$

is m independent.

V. ABERRATIONS

In this section we will try to estimate the relevance of the chromatic, “isotopic,” and spherical aberration. Other sources of aberration, like the one caused by fluctuations of the detuning, can be analyzed essentially in the same manner. Spontaneous aberration, on the other hand, is beyond the scope of this paper. We will also relax the conditions imposed so far on the profiles of the light and the atomic beam. We will concentrate on the region close to the z axis where, according to Eq. (4.10), classical and quantal foci nearly coincide.

A. Chromatic aberration

Chromatic aberration arises from the velocity spread in the incident atomic beam. The momentum correlations in a realistic matter wave beam have not been conclusively determined until now [21]. Our initial assumption that z can simply be parametrized by $v_z t$ tacitly implied that we are modeling the atomic motion along z with a plane wave traveling at velocity v_z . In such a context the velocity spread in the atomic beam is described by an incoherent mixture of plane waves with different velocities. This means that different atoms will have different interaction times with the light field, which produces a corresponding smearing of the focal spot. Let us consider a velocity shift $v_z \rightarrow v_z + \delta v_z$ and its consequence $z_n^F \rightarrow z_n^F + \delta z_n^F$:

$$\delta z_n^F \approx \delta v_z \frac{dz_n^F}{dv_z} = \delta v_z T \left[\frac{2z_n^F}{L} + \frac{1}{\sin^2 \varphi_n} \right]. \quad (5.1)$$

Since we are only interested in real foci, the expression in square brackets is always positive and unfortunately the lens cannot be made achromatic by a suitable choice of parameters.

B. Isotopic aberration

When the atomic species used in the beam consists of various isotopes, the exact focal positions will vary according to the different atomic masses. Since it is the momentum Mv_z which defines the de Broglie wavelength of the particles, this aberration is in fact part of the chromatic one.

We will not consider isotopic shifts of ω_a and we will assume that the velocity preparation is mass independent. Then a shift δM of the atomic mass will cause a position shift,

$$\delta z_n^F \approx \delta M \frac{dz_n^F}{dM} = \frac{\delta M}{2M} L \left[\frac{z_n^F}{L} + \frac{1}{\sin^2 \varphi_n} \right], \quad (5.2)$$

of the n th focus. This aberration can obviously be removed by employing isotopically pure sources. On the other hand, if

quantum focusing turns out to be a feasible method for lithography, the isotopic aberration could be used for creating gratings with lines made of alternating isotopes.

C. Spherical aberration

If we wanted to evaluate the spherical aberrations due to the anharmonicity of the optical potential in the general case, we would have to solve the quantum dynamical problem at least up to the quartic term of $|g|^2$. However, this problem is not much simpler than the original one with the full sinusoidal potential, whose analysis requires Mathieu functions and introduces energy-band structures.

Here instead we will limit ourselves to thin lenses and establish a simple connection with the results given in [15]. There the thin-lens condition is assumed from the very beginning and it therefore makes sense to expand Eq. (3.1) up to quadratic order around $x = \kappa$ instead of $x = 0$. Now observe that for ideal lenses like the one we analyzed so far, the origin for the Taylor expansion is irrelevant, since any quadratic expansion always reproduces the original parabola identically. This statement does not hold anymore if there are any deviations from the perfect harmonic shape. For instance, the expansion of $|g|^2$ from Eq. (3.1) up to quadratic order around $x = \kappa$ defines a new harmonic-oscillator problem with a shifted angular frequency

$$\omega_n^2 + \delta\omega_n^2 = \omega_n^2 \cos\left(\frac{4\pi\kappa}{\lambda}\right), \quad (5.3)$$

i.e.,

$$\delta\omega_n^2 = -\frac{\omega_n^2}{2} \left(\frac{4\pi\kappa}{\lambda}\right)^2, \quad (5.4)$$

and whose center is (within the same approximation) displaced away from zero by an amount

$$-\frac{\kappa}{3} \left(\frac{4\pi\kappa}{\lambda}\right)^2. \quad (5.5)$$

The anharmonicity of the true potential thus produces a shift δz_n^F in the focal positions given by

$$\delta z_n^F = \frac{1}{\varphi_n^2} \left(\frac{4\pi\kappa}{\lambda}\right)^2 \frac{L}{2}. \quad (5.6)$$

At the price of becoming increasingly useless for larger φ_n , the treatment in [15] is therefore superior in the thin-lens limit, since it automatically includes spherical aberration effects.

D. Gaussian light beams

So far we have assumed a flat-topped laser intensity profile. Sharp edges are, however, never realized in actual experiments, neither in pulsed nor in cw configurations [22]. Usually the turning on of the coupling (3.1) is modeled by some smooth function f that describes the cross-sectional shape of the laser beam

$$g(x, z = v_z t) = f(t) G \sin\left(\frac{2\pi x}{\lambda}\right). \quad (5.7)$$

It has been shown [23] that our results remain true for any f , as long as the turning on is adiabatic and the time variable t is replaced by $\tau = \int dt f^2(t)$. If we thus take a Gaussian $f(t) = \exp[-(t/T)^2]$ instead of a square field profile [$f(t) = 1$ for a time T] and if the assumption of adiabatic conditions is justified, we only have to change the parametrization of time accordingly and make sure that the region of interest is well outside the interaction area, so that the two descriptions essentially coincide. In particular, this will be the case in the example (using Cs atoms) given below.

E. Rectangular slits

Originally we introduced a Gaussian slit of width d because it simplified the mathematical treatment and allowed a simple understanding of the focusing dynamics. In a real experiment, however, such a slit will have a rectangular profile and will give rise to a more complex quantum focal pattern. The problem can still be solved analytically if expressed in terms of Fresnel integrals, but the somewhat technical details will be reported elsewhere. In very close analogy to the situation depicted in Fig. 3–6 of [18], the fundamental processes do not change, but plots of the focal shape like Fig. 2(a) acquire additional structure in the x direction.

In the next chapter we analyze a case which is symmetrical with respect to the atomic beam axis. Secondary structures due to sharp edges of the entrance slit do not influence the general results obtained there.

VI. OBSERVABILITY OF QUANTUM FOCUSING

We will assume now that $\kappa = 0$ and $\varphi = 0$, so that the quantum focal curve becomes a straight line along the z axis. The probability density of finding the atom at the position $x, z = v_z t$ irrespective of its internal state is then given by

$$\begin{aligned} & \sum_{j=-,+} \sum_{n=0}^{\infty} |\langle j, n, x', t | \psi \rangle|^2 \\ &= \sum_{n=0}^{\infty} \frac{|w_n|^2}{\sqrt{\pi} D_n(t)} \exp\left\{-\left[\frac{x'}{D_n(t)}\right]^2\right\}. \end{aligned} \quad (6.1)$$

Under which circumstances can the individual foci be observed? Along the atomic beam axis $x' = 0$ the above expression can be explicitly written as

$$\frac{1}{\sqrt{\pi} d} \sum_{n=0}^{\infty} |w_n|^2 \frac{(\cos^2 \varphi_n + \alpha^2 \varphi_n^2 \sin^2 \varphi_n)^{1/2}}{\sqrt{\left[\frac{\cos^2 \varphi_n + \alpha^2 \varphi_n^2 \sin^2 \varphi_n}{\alpha} \frac{t - t_n^{\text{QF}}}{T}\right]^2 + 1}}, \quad (6.2)$$

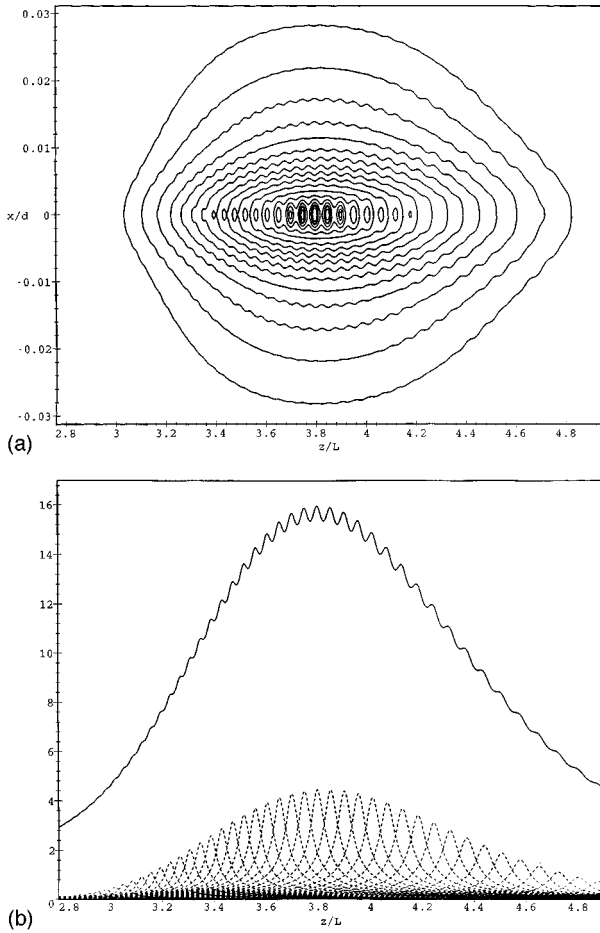


FIG. 2. Focal distribution for the parameters given in the text and $\langle a^\dagger a \rangle = 81$. Plot (a) shows contours of constant atomic probability density in the x - z plane. In (b) a cut along $x' = 0$ is shown. The wiggled curve is the sum over the individual quantum foci corresponding to each photon number n (dotted lines). The ordinate is in units of $1/d$.

which shows that in order to get clearly separated peaks, the expression in square brackets has to satisfy the condition

$$\frac{\cos^2 \varphi_n + \alpha^2 \varphi_n^2 \sin^2 \varphi_n}{\alpha} \cdot \frac{|t_{n-1}^{\text{QF}} - t_n^{\text{QF}}|}{T} \gg 1. \quad (6.3)$$

In addition we have to guarantee that the effective Hamiltonian description is applicable. This will be the case if the detuning is made so large, that the inequality

$$\left(\frac{\Delta}{2}\right)^2 \gg G^2 \langle a^\dagger a \rangle \quad (6.4)$$

holds. If one introduces typical, experimentally reasonable values for the atomic mass M (several AMU), the interaction time T (several 10^{-8} s), the coupling constant G (some 10^5 s $^{-1}$), the (optical) wavelength λ and the slit width d (some fraction of $\lambda/2$), one finds that the condition (6.3) is most easily fulfilled in the thin-lens regime. If we thus assume $\varphi_n \ll \pi/2$ and approximate $t_n^{\text{QF}} - t_{n-1}^{\text{QF}} \approx dt_n^{\text{QF}}/dn$, the visibility criterion (6.3) becomes essentially n independent and reads

$$\left(\frac{2\pi d}{\lambda}\right)^2 \frac{2G^2 T}{(-\Delta)} \gg 1. \quad (6.5)$$

This expression does not contain the atomic mass and depends on the wavelength only via the adjustable ratio d/λ . If we now, for instance, set $-\Delta/2 \equiv 3G\sqrt{\langle a^\dagger a \rangle}$, we find that the foci will only be distinguishable if G is very large and the photon number comparatively low [24]. We now want to quantify this statement.

We present a calculation based on the parameters of Ref. [25]. There the extremely high value of $G/2\pi = 20$ MHz is achieved by coupling the $(6S_{1/2}, F=4, M_F=4) \rightarrow (6P_{1/2}, F'=5, M'_F=5)$ transition of the D_2 line of Cs at $\lambda = 852$ nm to a high-finesse optical cavity. The atomic mass M is 2.26×10^{-25} kg and T equals seven (free) spontaneous lifetimes $\tau_s = 32$ ns. Using these values a maximal number of separable quantum focal peaks can be estimated [26].

Figure 2 shows the atomic density along the z axis for a Poissonian (coherent) photon distribution with $\langle a^\dagger a \rangle = 81$ and the detuning $-\Delta = 54 \times G$, when $d = \lambda/3$. The individual foci are clearly separated in this graph, which however represents idealized experimental conditions. We will now consider the effect of aberrations and the observational requirements they impose.

A (small) nonzero κ or φ offset is not critical, since it only displaces the entire focal pattern in the x - z plane. Fluctuations around these values can, however, wash out what we want to observe. Mechanical vibrations will cause varying incidence positions κ and shifts in both focal coordinates due to spherical aberration. Equating the interfocal distance (4.12) with the expression for the spherical aberration (5.6) one finds a maximal fluctuation amplitude $\hat{\kappa}$,

$$\hat{\kappa} \approx \frac{\lambda}{2\pi\sqrt{2\langle a^\dagger a \rangle}}, \quad (6.6)$$

which for the given case equals 10.5 nm [the corresponding shift (5.5) along x can then be neglected]. This can readily be achieved using active stabilization techniques as in Ref. [8]. More problematical is rotational noise, which contributes to the fluctuations of φ . Although these only displace the foci laterally, the small focal width imposes very strict limitations on the fluctuation amplitude $\hat{\varphi}$. Indeed, if one equates x_n^{F}/d from Eq. (4.1) with $D_n(t_n^{\text{F}})$ in Eq. (4.5) one finds

$$\hat{\varphi} \approx \hbar/d, \quad (6.7)$$

i.e., the atomic beam would have to be transversally cooled close to the one-photon recoil limit. Although this could in principle be achieved [27], it is probably unnecessary, as discussed below. In addition we have to consider rotational noise, and taking $\langle v_z \rangle = 310$ m/s from [25] we find maximally permissible rotational amplitudes of less than 10^{-2} mrad. In any case, the potential depth $\hbar G^2 \langle a^\dagger a \rangle / |\Delta| \approx 0.11$ μ eV limits the initial lateral velocity to a value below 0.4 m/s. Only one Cs isotope is present in the atomic beam. Chromatic aberration is therefore just a consequence of its longitudinal velocity spread. Using Eq. (5.1) one finds that velocity ratios $v_z/\delta v_z$ of 240 are necessary to avoid focal shifts larger than the average interfocal distance. Last but not least, we have to make sure the two-level model, on which

the whole theory is based, can be applied. Experimentally this could, for instance, be achieved by the method demonstrated in [28].

Several methods can be visualized for observing the focal structure. It has been proposed to use quantum focusing as a lithographical technique, by placing a substrate along the focal line and letting the atomic beam enter the standing light field with a lateral offset κ [14]. It is not obvious, however, that such a configuration would measure the focal curve given above, since it represents quite a different physical situation: a substrate placed along $x=0$ behind the interaction region is a boundary condition that should be included as part of the problem from the very beginning. A less invasive approach would be scanning the focal area with a probe laser parallel to the y axis. One could also try to use the quasiperiodicity of the focal structure as an intensity grating and observe the diffraction it produces on an incoming electromagnetic wave. The periodicity becomes better as $\langle a^\dagger a \rangle$ is increased and using the atomic velocity of the above example, its wavelength is found to be in the optical regime. The dimensions of the structure in the x direction are, however, much smaller than the diffractive focal spot size of an eventual probe beam. A way out of this problem could be *making use* of the aberration caused by fluctuations of φ . Since these do not change z_n^F , the net effect would be widening the focal spot widths. Also the lithographic method would be insensitive to such fluctuations. Less stringent conditions on the beam temperature would at the same time increase the amount of available atomic flux.

But even with such an untypically high coupling constant as we have considered here, not many more than ~ 100 photons could be resolved. Figure 3 shows the focal shape for an average number of 196 photons ($-\Delta=84 \times G$) and all other parameters unchanged. Even in the absence of any aberrations the focal structure due to light quantization can hardly be seen and it gets completely washed out in the classical limit.

VII. SUMMARY

The focusing behavior of a perfect dipole lens for atoms is decomposed into classical and quantum-mechanical features.

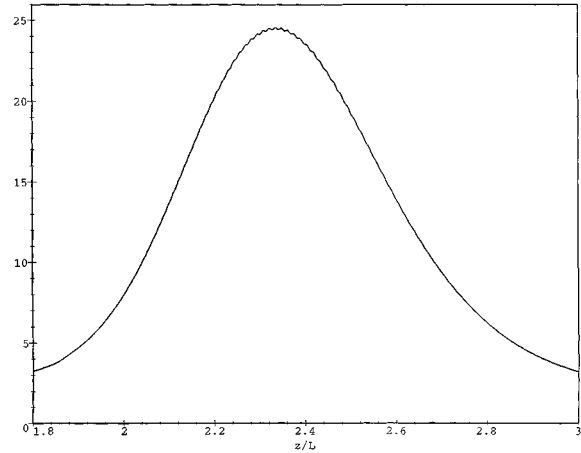


FIG. 3. Focal distribution along the z axis for the same parameters as in Fig. 2 but $\langle a^\dagger a \rangle = 196$ (and $-\Delta = 84 \times G$). Already for this average photon number the individual foci are hardly discernible.

In the thick-lens regime we predict a transition from convergent to divergent classical lens behavior. On the quantum level a simple and nontrivial expression describing the focal distribution is found. We discuss different sources of aberration and estimate under which circumstances the quantum nature of light leaves a visible trace in the quantum focal shape. We plan to include spontaneous emission and to verify up to which point adiabatic conditions are fulfilled when a more realistic laser beam profile is assumed in a quantum Monte Carlo simulation. A sinusoidal standing wave will be used and Doppler shifts considered.

ACKNOWLEDGMENTS

B.R. would like to thank J. C. Retamal for many useful discussions. This work was supported by FONDECYT Grant No. 2950068 and No. 1950801.

-
- [1] H. Friedburg and W. Paul, *Naturwissenschaften* **38**, 159 (1951); H. Friedburg, *Z. Phys.* **130**, 493 (1951).
 - [2] V. I. Balykin, V. S. Letokhov, Yu. B. Ovchinnikov, and A. I. Sidorov, *J. Mod. Opt.* **35**, 17 (1988).
 - [3] O. Carnal, M. Sigel, T. Sleator, H. Takuma, and J. Mlynek, *Phys. Rev. Lett.* **67**, 3231 (1991).
 - [4] W. G. Kaenders, F. Lison, A. Richter, R. Wynands, and D. Meschede, *Nature* **375**, 214 (1995).
 - [5] J. E. Bjorkholm, R. R. Freeman, A. Ashkin, and D. B. Pearson, *Phys. Rev. Lett.* **41**, 1361 (1978).
 - [6] V. I. Balykin and V. S. Letokhov, *Opt. Commun.* **64**, 151 (1987); G. M. Gallatin and P. L. Gould, *J. Opt. Soc. Am. B* **8**, 502 (1991); J. J. McClelland and M. R. Scheinfein, *ibid.* **8**, 1974 (1991).
 - [7] T. Sleator, T. Pfau, V. Balykin, and J. Mlynek, *Appl. Phys. B* **54**, 375 (1992).
 - [8] G. Timp, R. E. Behringer, D. M. Tennant, and J. E. Cunningham, *Phys. Rev. Lett.* **69**, 1636 (1992).
 - [9] J. J. McClelland, R. E. Scholten, E. C. Palm, and R. J. Celotta, *Science* **262**, 877 (1993); R. E. Scholten, J. J. McClelland, E. C. Palm, A. Gavrin, and R. J. Celotta, *J. Vac. Sci. Technol. B* **12**(3), 1847 (1994).
 - [10] K. K. Berggren, M. Prentiss, G. L. Timp, and R. E. Behringer, *J. Opt. Soc. B* **11**, 1166 (1994); J. J. McClelland, *ibid.* **12**, 1761 (1995).
 - [11] R. Gupta, J. J. McClelland, Z. J. Jabbour, and R. J. Celotta, *Appl. Phys. Lett.* **67**(10), 1378 (1995).
 - [12] R. Gupta, J. J. McClelland, P. Marte, and R. C. Celotta, *Phys. Rev. Lett.* **76**, 4689 (1996).

- [13] M. K. Olsen, T. Wong, S. M. Tan, and D. F. Walls, *Phys. Rev. A* **53**, 3358 (1996).
- [14] I. Sh. Averbukh, V. M. Akulin, and W. P. Schleich, *Phys. Rev. Lett.* **72**, 437 (1994).
- [15] E. Mayr, D. Krähler, A. M. Herkommer, V. M. Akulin, W. P. Schleich, and I. Sh. Averbukh, *Proceedings of Quantum Optics III [Acta Phys. Pol.]* **86**, 81(1994).
- [16] The experimental situation which most closely resembles the system we analyze here is described in T. Sleator, T. Pfau, V. Balykin, O. Carnal, and J. Mlynek, *Phys. Rev. Lett.* **68**, 1996 (1992), in the limit of high detuning.
- [17] See, for instance, S. Dyrting and G. J. Milburn, *Phys. Rev. A* **49**, 4180 (1994).
- [18] R. P. Feynman and A. R. Hibbs, *Quantum Mechanics and Path Integrals* (McGraw-Hill, New York, 1965), pp. 47–56.
- [19] B.-G. Englert, C. Miniatura, and J. Baudon, *J. Phys. (France) II* **4**, 2043 (1994).
- [20] See, for example, D. S. Saxon, *Elementary Quantum Mechanics* (Holden-Day, San Francisco, 1968), pp. 144–147. The algebra becomes especially simple if Eq. (3.7) is interpreted as a squeezed state.
- [21] For a thorough discussion see, for instance, R. Rubenstein, Term Paper (for a class in Atomic Physics), Massachusetts Institute of Technology, 1995 (unpublished).
- [22] See, for instance, P. E. Moskowitz, P. L. Gould, and D. Pritchard, *J. Opt. Soc. Am. B* **2**, 1784 (1985); D. Pritchard and P. L. Gould, *ibid.* **2**, 1799 (1985).
- [23] A. Dulčić, J. H. Eberly, H. Huang, J. Javanainen, and L. Rosso-Franco, *Phys. Rev. Lett.* **56**, 2109 (1986); P. L. Gould, G. A. Ruff, and D. E. Pritchard, *ibid.* **56**, 827 (1986).
- [24] Increasing the interaction time may help as well, but the growing influence of diffusive processes on the deterioration of fringe visibility is not easy to foresee. The best compromise between large T and a small spontaneous aberration may be found empirically by gradually slowing down the atomic beam.
- [25] Q. A. Turchette, C. J. Hood, W. Lange, H. Mabuchi, and H. J. Kimble, *Phys. Rev. Lett.* **75**, 4710 (1995).
- [26] We do not claim here that the particular setup described in [25] can be used for this purpose. In particular, a significant birefringence of the cavity prevents the realization of two-state atomic dynamics, as mentioned, in H. Mabuchi, Q. A. Turchette, M. S. Chapman, and H. J. Kimble, *Opt. Lett.* **21**, 1393 (1995).
- [27] Cooling of Cs atoms below the one-photon recoil limit has been demonstrated in traps. See, for instance, C. Salomon, J. Dalibard, W. D. Phillips, A. Clairon, and S. Guellati, *Europhys. Lett.* **12**(8), 638 (1990); K. Gibble and S. Chu, *Phys. Rev. Lett.* **70**, 1771 (1993).
- [28] P. L. Gould, G. A. Ruff, P. J. Martin, and D. E. Pritchard, *Phys. Rev. A* **36**, 1478 (1987).